Reduction of thermal conductivity by surface scattering of phonons in periodic silicon nanostructures

Roman Anufriev,[1] Jeremie Maire,[1,2] and Masahiro Nomura[1,3,4,*]

[1]*Institute of Industrial Science, the University of Tokyo, Tokyo 153-8505, Japan*

[2]*Laboratory for Integrated Micro Mechatronic Systems, National Center for Scientific Research-Institute of Industrial Science (LIMMS/CNRS-IIS), the University of Tokyo, Tokyo 153-8505, Japan*

[3]*Institute for Nano Quantum Information Electronics, the University of Tokyo, Tokyo 153-8505, Japan*

[4]*PRESTO, Japan Science and Technology Agency, Saitama 332-0012, Japan*

(Received 9 September 2015; revised manuscript received 30 October 2015; published 12 January 2016)

We investigate the impact of various phonon-scattering mechanisms on the in-plane thermal conductivity of suspended silicon thin films with two-dimensional periodic arrays of holes, i.e., phononic crystal (PnC) nanostructures. A large amount of data on the PnC structures with square, hexagonal, and honeycomb lattices reveals that the thermal conductivity is mostly determined by the surface-to-volume ratio. However, as the characteristic size of the structure is reduced down to several tens of nanometers, thermal conductivity becomes independent of the surface-to-volume ratio, lattice type, and other geometrical parameters, being controlled solely by the distance between adjacent holes (neck size).

DOI: 10.1103/PhysRevB.93.045411

I. INTRODUCTION

Nanoscale structures are regarded as potential building blocks for future thermoelectric devices [1,2] due to the possibility of achieving efficient heat-to-electricity conversion in silicon [3,4]. Indeed, nanopatterning significantly reduces the thermal conductivity of the material [5–7], leaving its electrical conductivity almost unaffected [5,8]. In the past decade, it has been demonstrated experimentally that the thermal conductivity of silicon nanowires [4,6] and thin films [9–12] decreases as the limiting dimension (thickness or diameter) is decreased, and manyfold reduction of thermal conductivity relative to the value in the bulk can be easily achieved. Recent experiments showed that further reduction of thermal conductivity is possible by nanopatterning of the thin films: The works of Yu *et al.* [5] and Tang *et al.* [13] demonstrated reduction of thermal conductivity by one order of magnitude in thin films patterned with periodic arrays of holes compared to unpatterned thin films of the same thickness. However, this high reduction can partly be explained by the surface roughness, which alone can reduce the thermal conductivity by one order of magnitude [4]. Indeed, recent works by Nomura and co-workers on similar periodic nanostructures [14] and nanowires [6] with relatively low surface roughness demonstrated moderate reduction of thermal conductivity by nanopatterning.

Several different processes can affect heat transfer at the nanoscale: phonon scattering at impurities [4], three-phonon scattering processes [15,16], and grain or surface boundary scattering [14,15], which, in particular, is strongly dependent on surface roughness. When the phonons lose their phase after such scattering events, these processes are often referred to as "incoherent" scattering mechanisms, in contrast to "coherent" scattering in which the phase is preserved [17]. The preservation of phase by phonons in periodic nanostructures leads to wave interference of the thermal phonons, thus affecting the phonon dispersion relation and, as a consequence, changing the heat conduction properties of the material. In this case, such periodic structures are called phononic crystals (PnCs) as acoustic analogs of photonic crystals. The impact of the coherent scattering on thermal conduction has been experimentally demonstrated only at sub-Kelvin temperatures [18,19] where phonon wavelengths are longer than the characteristic size of the structure and can thus be scattered coherently. However, even at room temperature, many authors have tentatively attributed the low experimental values of thermal conductivity in PnC nanostructures to the impact of coherent scattering [5,20,21]. On the other hand, it is often argued that at room temperature phonons mostly scatter incoherently [22–26] because surface roughness destroys the coherence of short-wavelength phonons [27]. In general, the exact roles of various processes that determine the thermal conductivity of nanostructures at different temperatures remain unknown, and the variety of scattering mechanisms results in a range of possible experimental result interpretations. Therefore, the impact of coherent and incoherent scattering mechanisms on thermal conductivity is one of the hottest topics in nanoscale heat transport.

In the present paper, we aim to clarify the roles of coherent and incoherent phonon boundary scattering mechanisms and highlight a "bottleneck" phenomenon appearing in the narrow regions of nanostructures. In contrast to electrically based measurement techniques, our measurement system is optical and thus does not require any wire bonding or special treatment of each sample. This allows us to fabricate and measure a large number of structures on the same chip, which makes this comparative study possible.

II. SAMPLE DESCRIPTION

To study nanoscale heat transport, we use suspended thin silicon membranes with periodic arrays of holes. Figure 1(a) shows a schematic of a typical suspended PnC nanostructure. To fabricate such structures, we used a commercially available (100) silicon-on-insulator wafer with an 80-nm-thick upper

*nomura@iis.u-tokyo.ac.jp

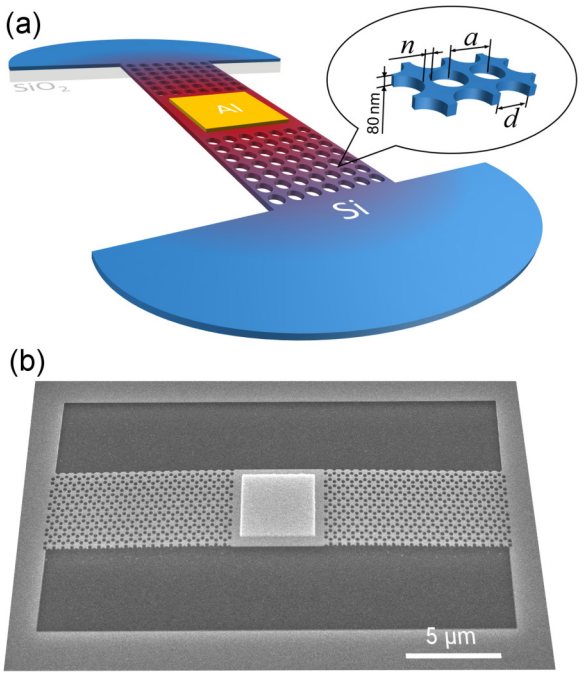

FIG. 1. (a) Schematic of a suspended PnC structure. (b) SEM image of a typical structure with a honeycomb lattice ($a = 280$ and $d = 228$ nm).

monocrystalline silicon layer and a 400-nm-thick SiO_2 buried layer. Prior to nanostructure fabrication, we deposited a 125-nm-thick 4×4-μm^2 Al pad that serves as a heater. Then, the PnC nanostructures were formed via electron-beam lithography using a reactive ion etching/inductively coupled plasma system with SF_6/O_2 gas as the etchant. The oxide layer under the silicon layer was removed with hydrofluoric acid in order to suspend the structures. The width and the length of the entire suspended structure are 5 and 25 μm, respectively. In addition, we also fabricated two unpatterned suspended membranes with thicknesses of $h = 80$ and 145 nm.

Figure 1(b) shows a scanning electron microscopy (SEM) image of a typical suspended silicon membrane with two-dimensional periodic arrays of holes. In this paper, we consider PnCs of three different lattices: square, hexagonal, and honeycomb. For each lattice type, we fabricated a number of structures with periods of 120, 160, 200, 240, and 280 nm and several different diameters of holes for each period. In total, about 30 structures were fabricated for each lattice type. SEM images of typical structures with periods of 160 nm [Fig. 2(a), 2(c), and 2(e)] and 280 nm [Fig. 2(b), 2(d), and 2(f)] demonstrate good alignment of well-circular holes with surface roughness not exceeding a few nanometers.

III. EXPERIMENTAL DATA

To measure the in-plane thermal conductivity of our samples, we used the micro-time-domain thermoreflectance (μ-TDTR) method [14,28], similar to the classical TDTR [29]. In this pump-probe experimental technique the reflectance of the Al pad is monitored over time with a continuous-wave laser (probe) beam, whereas a pulse laser (pump) beam periodically

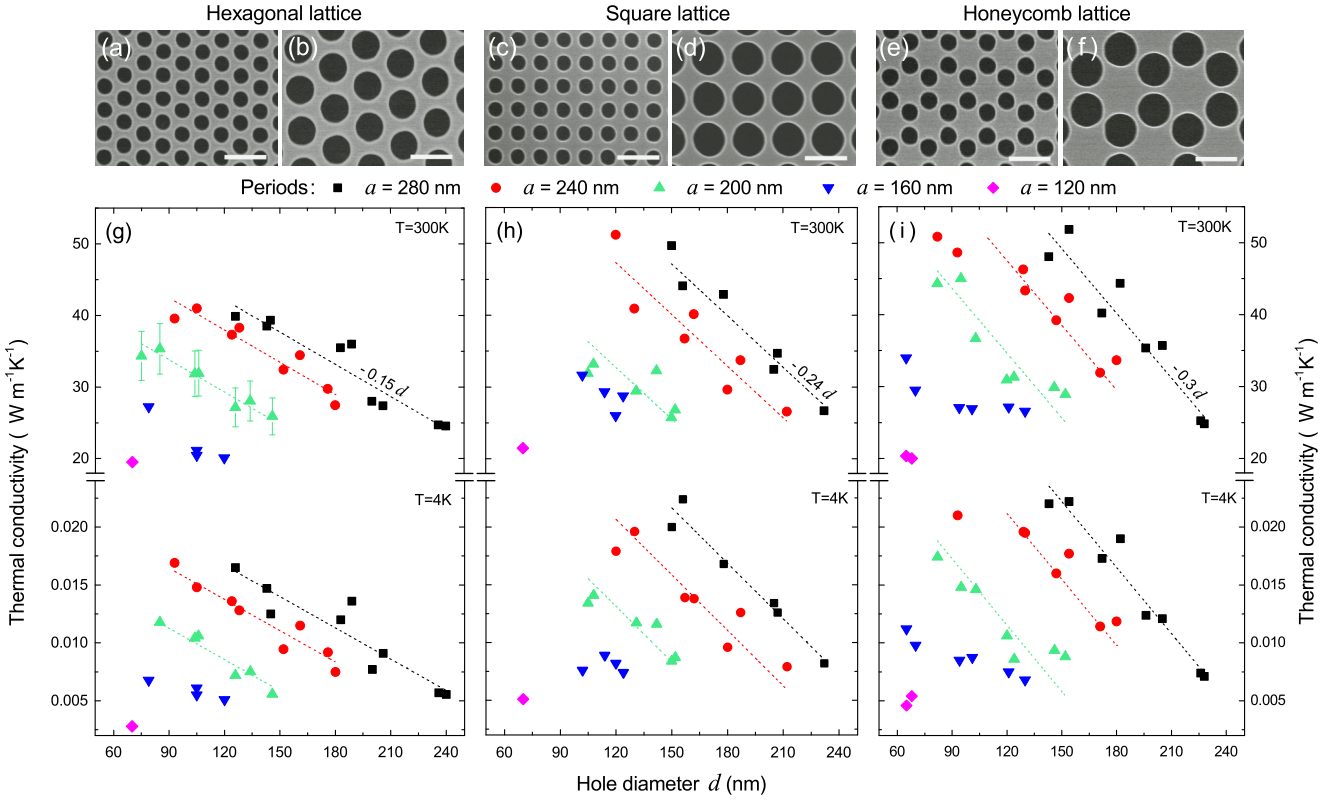

FIG. 2. (a)–(f) SEM images of structures with periods of 160 and 280 nm for each lattice (scale bars are 300 nm). Thermal conductivities of the PnC structures of (g) hexagonal, (h) square, and (i) honeycomb lattice types with different periods as a function of hole diameter at the temperatures of 300 and 4 K. The dashed lines are linear fits.

applies heat to the surface of the pad. The change in the reflectance, caused by the heating, can be linked to the change in the temperature of the pad through the thermoreflectance coefficient, and thus the rate of the heat dissipation in the structure can be measured. To extract the values of thermal conductivity, we fit our experimental data simulating the same experiment in the same structures via the finite element method implemented by COMSOL MULTIPHYSICS®, using the thermal conductivity of the PnC region as a free parameter. A detailed explanation of this measurement technique is available in the Supplemental Material [30]. The inaccuracy of our thermal conductivity data is estimated to be less than 5%–10%, whereas the errors of the SEM measurements do not exceed 2–4 nm (see the Supplemental Material [30]).

Figures 2(g)–2(i) show thermal conductivities of PnCs with different periods and lattice types as a function of hole diameter at the temperatures of 300 and 4 K. As a rule, for any given hole diameter, the structures of each lattice type demonstrate a lower thermal conductivity when the period is lower. Meanwhile, for any given period, thermal conductivity decreases as the hole size is increased. We fit these decreasing trends with linear functions using inclination factors constant for each lattice (dashed lines). These trends significantly differ from one lattice to another: the smallest inclination is observed in the hexagonal lattice, whereas the honeycomb lattice shows the steepest trends. In general, the results at room and low temperatures are very similar. To gain more understanding of the mechanisms behind our experimental data we plot the ratio of thermal conductivity of PnC structures to that of the unpatterned membrane ($\kappa_{\mathrm{PnC}}/\kappa_{\mathrm{Membrane}}$) as a function of diameter-to-period ratio in honeycomb structures at 300 K [Fig. 3(a)] (plots for other lattice types are available in the Supplemental Material [30]). The data for the structures of long periods ($a = 240$ and 280 nm) seem to follow the same trend and are close to the prediction of the Eucken model [31]: $\kappa_{\mathrm{PnC}}/\kappa_{\mathrm{Membrane}} = (1-\varphi)/(1+\varphi/2)$, where φ is the porosity of the structure. This fact may suggest that in our structures the mean free path (MFP)—the maximum distance that a phonon can travel until an incoherent scattering event—is already significantly limited by the thickness of the membrane (80 nm) as demonstrated by Wang and Huang [32] and can be limited further only when the neck size (n) of the structure becomes less than the membrane thickness [14]. In the next sections we will discuss various mechanisms which control heat transport and limit phonon MFP on the nanoscale.

IV. COHERENT SURFACE SCATTERING

Let us now consider various types of phonon scattering in our samples. Since the samples were fabricated from an undoped monocrystalline silicon chip, we do not expect strong scattering at the impurities. The impact of three-phonon processes does not depend on geometry but temperature only [33] and is the same in different samples. Moreover, since all our samples were fabricated simultaneously on the same chip, we do not expect variations in surface roughness between different samples. Thus, only coherent and incoherent surface scattering mechanisms remain to explain the geometry dependence of thermal conductivity. Recently, we theoretically investigated the impact of phonon

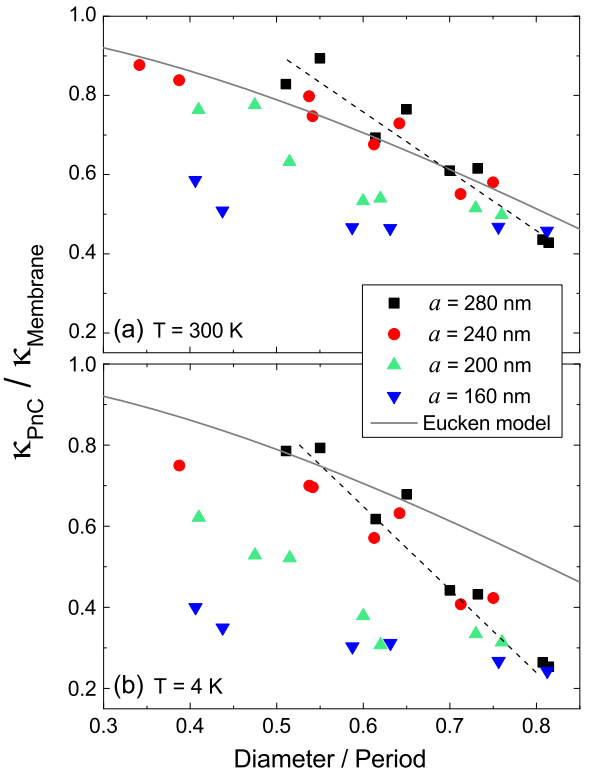

FIG. 3. Relative thermal conductivity of honeycomb structures with different periods as a function of diameter-to-period ratio at the temperatures of (a) 300 K and (b) 4 K. The dashed black lines are linear fits of the data on structures with $a = 280$ nm, and the solid gray lines show the prediction of the Eucken model.

dispersion modifications due to coherent scattering on the heat transfer in the same PnC nanostructures [34,35]. We found that coherent scattering reduces thermal conductivity of PnC structures as compared to unpatterned membranes, and this reduction is similar in all three lattices and becomes more significant as the diameter-to-period ratio increases. To see if our experimental data agree with these predictions, we also plot relative thermal conductivity ($\kappa_{\mathrm{PnC}}/\kappa_{\mathrm{Membrane}}$) data at 4 K [Fig. 3(b)]. At low temperatures even the structures of the lowest diameter-to-period ratio systematically show that the values of $\kappa_{\mathrm{PnC}}/\kappa_{\mathrm{Membrane}}$ are 15%–20% lower than those at room temperature. As the diameter-to-period ratio is increased, the relative thermal conductivity is decreasing more steeply at 4 K than at room temperature (at least for the structures of long periods) as indicated by dashed lines in Fig. 3. The same trends were found for all three lattices (see the Supplemental Material [30]). This finding indicates that there may be a mechanism which further reduces thermal conductivity at 4 K and depends on diameter-to-period ratio. Since it is often assumed that coherent phonon scattering appears only at low temperatures and is negligible at room temperature [22–26], the coherent modifications of phonon dispersion can be one of the possible interpretations of our low-temperature observations. However, at 4 K the impact of the coherent scattering seems to be relatively weak (about 20%), whereas the reduction predicted theoretically is about an order of magnitude [34,35]. To explain this discrepancy we have to assume that only a low-frequency part of the phonon spectrum is affected by coherent scattering

even at 4 K, whereas most of the phonons are still scattered incoherently. Indeed, if we assume that only phonons with wavelengths longer than, for example, 100 nm (30 nm) can be scattered coherently, then calculating the phonon spectrum at 4 K using the technique from the Refs. [34,35], we can estimate that such coherently scattered phonons contain only about 10% (40%) of the whole spectrum. This estimation is also in agreement with the calculation by Marconnet *et al.* [36], which shows that the impact of coherent scattering would only start appearing at the temperatures below 10 K in the structures of approximately the size of ours. Moreover, this is also consistent with the results of our recent experimental study on disordered PnC: Signs of coherent scattering were observed only at the temperatures below 7 K, and the reduction of thermal conductivity, caused by the coherent scattering, was about 15% at 4 K [37]. However, all the features discussed above could also be interpreted as a result of longer wavelengths of phonons at low temperatures and, as a consequence, stronger incoherent scattering by holes.

V. INCOHERENT SURFACE SCATTERING: SURFACE−TO−VOLUME RATIO

If the coherent scattering plays only a minor role in the heat transport at 4 K and probably a negligible role at room temperature, the only remaining explanation for our observations is incoherent surface boundary scattering. To understand how this scattering mechanism affects the thermal conductivity on the nanoscale we will approach this phenomenon from two sides: First we will discuss the role of the mere presence of scattering surfaces and then the impact of the geometry of the structure. The first point of view suggests that surface scattering rate is related to the amount of surface per unit volume [5,38,39]. For any given structure, this surface-to-volume (S/V) ratio depends on diameter, period, and lattice type of the structure. Here we do not distinguish top/bottom surfaces of the membrane and surfaces of the holes. In reality surfaces of the holes may have higher surface roughness, but we assume that the scattering is purely diffusive in both cases [32]. So if thermal conductivity is controlled only by the presence of a surface, i.e., regardless of placement of the surfaces, we may expect the same values of thermal conductivity for the structures with the same S/V ratio [5,40].

In Fig. 4(a), we plot the thermal conductivity for all the measured PnC structures and unpatterned membranes, together with literature values for unpatterned membranes [9–12,41,42] as a function of S/V ratio at room temperature. Here we selected literature data on the unpatterned membranes because patterned structures available in literature have significant surface roughness, so it is difficult to estimate their actual S/V ratio. All the structures show a reduction of thermal conductivity as the S/V ratio is increased. To summarize the scattered literature data, we drew a fit, which reflects a general trend. The unpatterned membranes, also measured in this paper ($\kappa = 58$ and 75 W m^{-1} K^{-1} for $h = 80$ and 145 nm correspondingly), are in fair agreement with the general trend, which demonstrates the reliability of our measurement technique. As far as PnC structures are concerned, all three lattices also seem to follow this general trend. Therefore, the order of thermal conductivity of nanostructures is probably

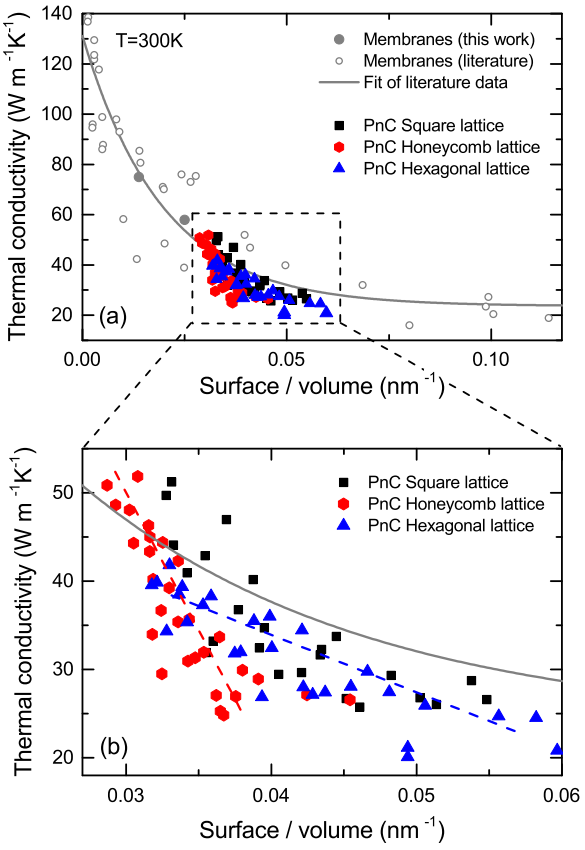

FIG. 4. Room-temperature thermal conductivities of PnC structures and unpatterned membranes measured in this paper and in Refs. [9–12,41,42] as a function of the S/V ratio. The gray line shows fit of the literature data. The dashed lines are guides to the eye.

mostly determined by the S/V ratio, regardless of placement of the scattering surfaces. The same idea is confirmed by theoretical work by Jeng *et al.* [40]: Thermal conductivity of various nanostructures is controlled by the S/V ratio rather than structure type, alignment, or size.

However, on closer inspection [Fig. 4(b)], PnCs of different lattices do not exhibit exactly the same trends. The structures with a honeycomb lattice, having low S/V ratio, demonstrate a steep decreasing trend, whereas the trend for the hexagonal lattice is flatter as indicated by dashed lines in Fig. 4(b); the square lattice, having an average S/V ratio, somewhat resembles the behavior of both. Moreover, despite the differences in the S/V ratio, all three lattices (except for a few points) seem to share the same minimum value of thermal conductivity ($\approx$25 W m^{-1} K^{-1}) for the extreme structures with the highest S/V ratio. A similar feature has also been demonstrated by Yu *et al.* [5] where the order of thermal conductivity in nanostructures was proportional to S/V ratio, yet an extremely small nanomesh structure demonstrated deviations from this trend.

VI. INCOHERENT SURFACE SCATTERING: NECKING EFFECT

These observations suggest the existence of a limiting factor that determines thermal conductivity in the structures with diameters close to the period, regardless of the lattice type.

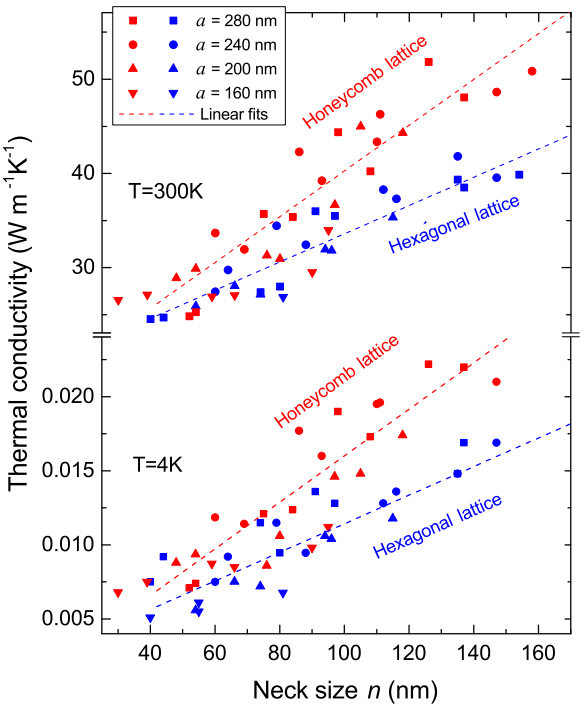

FIG. 5. Thermal conductivity of the structures with hexagonal (blue) and honeycomb (red) lattices as a function of the neck size at 300 and 4 K. The dashed lines are linear fits of the data.

One such factor can be the neck size (n) of the structure. A phenomenon, known as the "necking effect," has been suggested to explain the reduction of thermal conductivity in porous nanostructures with increasing pore diameter [6,13]. This effect suggests that, in the structures with relatively small neck sizes, the MFP can be limited by the size of the neck, which as a consequence reduces thermal conductivity. To demonstrate this effect, we plot thermal conductivities of all hexagonal and honeycomb structures as a function of the neck size [Fig. 5]. When the neck size is large, thermal conductivity of the structures with the honeycomb lattice is clearly higher than that of the structures with the hexagonal lattice. This fact can be explained simply by lower S/V ratio (or lower porosity) in the honeycomb lattice as compared to the hexagonal lattice due to the absence of every third hole. However, as the neck size decreases, all structures demonstrate very similar values of thermal conductivity regardless of the period, lattice type, and S/V ratio. This phenomenon is very similar at room and low temperatures and thus probably does not depend on phonon wavelength but can be understood in terms of MFP. It has been theoretically demonstrated that an increase in the diameter-to-period ratio can limit the maximum phonon MFP, thus limiting thermal conductivity [14,22]. Here, we have shown experimentally that this limitation probably originates from the reduction of the neck size rather than from other factors, such as placement of holes, the S/V ratio, or porosity.

VII. CONCLUSION

In conclusion, we have investigated the impact of various phonon scattering mechanisms on the thermal conductivity of PnC structures with different lattice types, periods, and hole diameters. From our room and low-temperature observations, we concluded that the additional reduction of thermal conductivity in PnC structures as compared to unpatterned membranes observed at the temperature of 4 K can be interpreted as a result of coherent scattering. This observation is consistent with our recent experimental results on disordered PnCs [37]. As far as incoherent scattering mechanisms are concerned, there are two main factors controlling thermal conductivity. The first factor is the reduction of thermal conductivity due to the mere presence of hole surfaces and boundaries of the membrane. In this case, thermal conductivity is controlled by the S/V ratio of the structure and does not depend on the placement of holes. The second factor, known as the necking effect, appears when the distance between hole edges becomes small. The neck limits the maximum phonon MFP, which determines the thermal conductivity of the structure regardless of its S/V ratio and other geometrical parameters. These results imply that nanopatterning of thin films affects thermal conductivity not only by the mere presence of an additional scattering surface, but also via various nanoscale phenomena, such as the necking effect and coherent phonon scattering, and further theoretical and experimental studies are required to gain a better understanding of these processes.

ACKNOWLEDGMENTS

This work was supported by the Project for Developing Innovation Systems of the Ministry of Education, Culture, Sports, Science and Technology (MEXT), Japan, Kakenhi (Grants No. 25709090 and No. 15K13270), and the Foundation for the Promotion of Industrial Science.

[1] M. Maldovan, Nature (London) **503**, 209 (2013).
[2] G. Schierning, Phys. Status Solidi A **211**, 1235 (2014).
[3] M. Haras, V. Lacatena, F. Morini, J.-F. Robillard, S. Monfray, T. Skotnicki, and E. Dubois, Mater. Lett. **157**, 193 (2015).
[4] A. I. Hochbaum, R. Chen, R. D. Delgado, W. Liang, E. C. Garnett, M. Najarian, A. Majumdar, and P. Yang, Nature (London) **451**, 163 (2008).
[5] J.-K. Yu, S. Mitrovic, D. Tham, J. Varghese, and J. R. Heath, Nat. Nanotechnol. **5**, 718 (2010).
[6] M. Nomura, J. Nakagawa, Y. Kage, J. Maire, D. Moser, and O. Paul, Appl. Phys. Lett. **106**, 143102 (2015).
[7] J. Lee, J. Lim, and P. Yang, Nano Lett. **15**, 3273 (2015).
[8] M. Nomura, Y. Kage, D. Müller, D. Moser, and O. Paul, Appl. Phys. Lett. **106**, 223106 (2015).
[9] P. Ferrando-Villalba, A F. Lopeandia, L. Abad, J. Llobet, M. Molina-Ruiz, G. Garcia, M. Gerbolès, F. X. Alvarez, A. R. Goñi, F. J. Muñoz-Pascual, and J. Rodríguez-Viejo, Nanotechnology **25**, 185402 (2014).

[10] E. Chávez-Ángel, J. S. Reparaz, J. Gomis-Bresco, M. R. Wagner, J. Cuffe, B. Graczykowski, A. Shchepetov, H. Jiang, M. Prunnila, J. Ahopelto, F. Alzina, and C. M. Sotomayor Torres, APL Mater. **2**, 012113 (2014).
[11] Y. S. Ju, Appl. Phys. Lett. **87**, 153106 (2005).
[12] W. Liu and M. Asheghi, Appl. Phys. Lett. **84**, 3819 (2004).
[13] J. Tang, H.-T. Wang, D. H. Lee, M. Fardy, Z. Huo, T. P. Russell, and P. Yang, Nano Lett. **10**, 4279 (2010).
[14] M. Nomura, Y. Kage, J. Nakagawa, T. Hori, J. Maire, J. Shiomi, R. Anufriev, D. Moser, and O. Paul, Phys. Rev. B **91**, 205422 (2015).
[15] W. Fon, K. C. Schwab, J. M. Worlock, and M. L. Roukes, Phys. Rev. B **66**, 045302 (2002).
[16] Y.-J. Han, Phys. Rev. B **54**, 8977 (1996).
[17] M. Maldovan, Nat. Mater. **14**, 667 (2015).
[18] N. Zen, T. A. Puurtinen, T. J. Isotalo, S. Chaudhuri, and I. J. Maasilta, Nat. Commun. **5**, 3435 (2014).
[19] I. J. Maasilta, T. A. Puurtinen, Y. Tian, and Z. Geng, J. Low Temp. Phys. (2015).
[20] S. Alaie, D. F. Goettler, M. Su, Z. C. Leseman, C. M. Reinke, and I. El-Kady, Nat. Commun. **6**, 7228 (2015).
[21] P. E. Hopkins, C. M. Reinke, M. F. Su, R. H. Olsson, E. A. Shaner, Z. C. Leseman, J. R. Serrano, L. M. Phinney, and I. El-Kady, Nano Lett. **11**, 107 (2011).
[22] A. Jain, Y.-J. Yu, and A. J. H. McGaughey, Phys. Rev. B **87**, 195301 (2013).
[23] E. Dechaumphai and R. Chen, J. Appl. Phys. **111**, 073508 (2012).
[24] R. Prasher, T. Tong, and A. Majumdar, Nano Lett. **8**, 99 (2008).
[25] C. Dames and G. Chen, J. Appl. Phys. **95**, 682 (2004).
[26] N. K. Ravichandran and A. J. Minnich, Phys. Rev. B **89**, 205432 (2014).
[27] J. M. Ziman, *Electrons and Phonons: The Theory of Transport Phenomena in Solids* (Clarendon, Oxford, 1962).
[28] J. Maire and M. Nomura, Jpn. J. Appl. Phys. **53**, 06JE09 (2014).
[29] D. G. Cahill, Rev. Sci. Instrum. **75**, 5119 (2004).
[30] See Supplemental Material at http://link.aps.org/supplemental/10.1103/PhysRevB.93.045411 for a detailed explanation of the measurement technique.
[31] A. Eucken and E. Kuhn, Z. Phys. Chem., Abt. A **134**, 193 (1928).
[32] X. Wang and B. Huang, Sci. Rep. **4**, 6399 (2014).
[33] M. Holland, Phys. Rev. **132**, 2461 (1963).
[34] R. Anufriev and M. Nomura, Phys. Rev. B **93**, 045410 (2016).
[35] R. Anufriev and M. Nomura, Phys. Rev. B **91**, 245417 (2015).
[36] A. M. Marconnet, T. Kodama, M. Asheghi, and K. E. Goodson, Nanoscale Microscale Thermophys. Eng. **16**, 199 (2012).
[37] J. Maire, R. Anufriev, H. Han, S. Volz, and M. Nomura, arXiv:1508.04574.
[38] A. J. Kulkarni and M. Zhou, Appl. Phys. Lett. **88**, 141921 (2006).
[39] D. M. Photiadis, J. Phys.: Conf. Ser. **92**, 012056 (2007).
[40] M.-S. Jeng, R. Yang, D. Song, and G. Chen, J. Heat Transfer **130**, 042410 (2008).
[41] M. Asheghi, Y. K. Leung, S. S. Wong, and K. E. Goodson, Appl. Phys. Lett. **71**, 1798 (1997).
[42] Y. S. Ju and K. E. Goodson, Appl. Phys. Lett. **74**, 3005 (1999).